SA: Gridding methods

Bottle data from the Pacific Ocean Interior Carbon Data Synthesis (PACIFICA) (Suzuki et al., 2013), the Global Ocean Data Analysis Program (GLODAP), and the Carbon Dioxide in the Atlantic Ocean (CARINA) datasets (Key et al., 2004; 2010) were obtained from the Carbon Dioxide Information and Analysis Center website and merged. The merged dataset was interpolated onto the World Ocean Atlas grid (Locarnini et al., 2010; Antonov et al., 2010; Garcia et al., 2010a,b). The interpolation procedure has several steps:

First the data from each station in these datasets are interpolated vertically onto the depth intervals used for the World Ocean Atlas using cubic Hermite piecewise polynomial interpolation. Interpolated data is thrown out if the nearest neighbors above and below the depth interval are further apart than the sum of one hundred meters and one tenth of the depth of the depth interval. No extrapolations are used.

Second, for an outlier check, the interpolated data from each depth surface is re-estimated using a Delaunay triangulation interpolant for 3-D linear interpolation with a factor of four up-scaling of latitude distances relative to longitude distances. The interpolant is constructed from all interpolated data from a given depth interval within 20° latitude and longitude with the exception the data point being re-estimated. These depth-and-horizontally-interpolated values are then compared to the depth-interpolated values to obtain statistics for the disagreement between the two sets. When the deviation of these two estimates exceeds four times the standard deviation for a property for any of the properties being interpolated, the interpolated data at that location is thrown out. This outlier removal process resulted in the loss of approximately 0.6% of all vertically interpolated data.

Third, data is interpolated horizontally onto the World Ocean Atlas latitude and longitude

grid for each depth surface using the same procedure used in the outlier check, but with the interpolants constructed from all remaining interpolated data from that depth surface.

Fourth, a weighting function equal to the inverse of the square of the distance between every point and every other point is used to reduce the impact of individual measurements. Distance contributions from latitude differences are again weighted four times as heavily as distance contributions from longitude differences. Additionally, latitude distances between points in different ocean basins are calculated by summing the latitude differences between each of the two points and the southern tip of South America (for Atlantic to Pacific distances) or Africa (for Atlantic to Indian distances). Weights indicating a data point is less than 120 nautical miles away from the location at which the value is being interpolated, either zonally or meridionally, are re-estimated assuming the data point is at least this distance away along this axis. All interpolated data at 0 meters depth is set equal to data interpolated at 10 meters depth..

Finally, *in situ* estimations of water mass density and aragonite and calcite saturation are estimated (for Figure 8 only) using the built in routines of the Ocean Data View software (Schlitzer, 2012), which in turn rely upon the density formulation of TEOS10 and the carbonate constants of Dickson et al. (2007).

Data from high and low longitudes (> 120° W and E) are mirrored on the opposite sides of the pre-interpolation datasets (i.e. at 180-240° E and W) to avoid map edge errors in all interpolation and smoothing steps. Data falling outside of the region bound by data are set equal to the value at the nearest point bound by the data.

SB: Uncorrected freshwater residual estimate

We estimate the size of the uncorrected residual from freshwater cycling by considering

seawater with an initial salinity S^i and potential alkalinity A_P^i that is diluted with non-alkaline freshwater, resulting in seawater with a final potential alkalinity A_P^f and salinity S^f. These values can be related with:

$$A_P^f = A_P^i \frac{S^f}{S^i} \quad \text{(SB1)}$$

Equations (5) and (SB1) can be combined and rearranged to estimate the size of the undesired *Alk** residual *r*:

$$r = \left(\frac{A_P^i}{S^i} - 66.4 \right) (S^f - S^i) \quad \text{(SB2)}$$

We divide this residual by the difference between A_P^f and A_P^i, substitute in Eq. (SB1), and rearrange to estimate the fraction *f* of the alkalinity change that is not removed by using *Alk**:

$$f = \frac{r}{A_P^f - A_P^i} = \frac{\frac{A_P^i}{S^i} - 66.4}{\frac{A_P^i}{S^i}} \quad \text{(SB3)}$$

The standard deviation of the potential alkalinity to salinity ratio from the 66.4 μmol kg^{-1} mean surface ratio (i.e. the standard value of the numerator in Eq. SB3) in our gridded dataset is 2.5% of our mean surface ratio (i.e. the denominator in Eq. SB3). This suggests *Alk** typically removes 97.5% of the freshwater cycling influence on the marine alkalinity distribution. The standard value of *r* is less than 1% of the standard deviation of global *Alk** (53.5 μmol kg^{-1} in our gridded data product, see Appendix), so this residual has little influence on the global *Alk** distribution.

SC: Derivation of tracer, demonstration of conservation, and comparison to an alternative

In this section we demonstrate the critical point that our tracer, unlike traditionally

normalized alkalinity, mixes conservatively and responds linearly to sources and sinks for alkalinity. We begin with the generalized form for the conservation equation for a tracer *C*:

$$\frac{\partial C}{\partial t} - \left.\frac{\partial C}{\partial t}\right|_{\text{advection}} - \left.\frac{\partial C}{\partial t}\right|_{\text{diffusion}} = SMS(C) \qquad \text{(SC1)}$$

Here *SMS*(C) is shorthand for "sources minus sinks of C." We assume a fixed volume filled with incompressible seawater and write out this equation for alkalinity and salinity:

$$\frac{\partial S}{\partial t} + \mathbf{U}\cdot\nabla S + \nabla\cdot(D\nabla S) = SMS(S) \;\; , \;\; \frac{\partial A}{\partial t} + \mathbf{U}\cdot\nabla A + \nabla\cdot(D\nabla A) = SMS(A) \quad \text{(SC2,SC3)}$$

We assume that there are no sources or sinks for salinity:

$$\frac{\partial S}{\partial t} + \mathbf{U}\cdot\nabla S + \nabla\cdot(D\nabla S) = 0 \qquad \text{(SC4)}$$

We rearrange the alkalinity equation to be similarly equal to zero:

$$\frac{\partial A}{\partial t} + \mathbf{U}\cdot\nabla A + \nabla\cdot(D\nabla A) - SMS(A) = 0 \qquad \text{(SC5)}$$

Here we multiply equation (SC4) by the ratio of the average value of the alkalinity relative to the average value of the salinity in the surface ocean. We then set this equation equal to (SC5) to obtain:

$$\frac{\partial A}{\partial t} + \mathbf{U}\cdot\nabla A + \nabla\cdot(D\nabla A) - SMS(A) = \frac{\overline{A}}{\overline{S}}\left(\frac{\partial S}{\partial t} + \mathbf{U}\cdot\nabla S + \nabla\cdot(D\nabla S)\right) \qquad \text{(SC6)}$$

This can be rearranged to obtain:

$$\frac{\partial A}{\partial t} - \frac{\overline{A}}{\overline{S}}\frac{\partial S}{\partial t} + \mathbf{U}\cdot\nabla\cdot\left(A - \frac{\overline{A}}{\overline{S}}S\right) + \nabla\cdot(D\nabla\cdot\left(A - \frac{\overline{A}}{\overline{S}}S\right) = SMS(A) \qquad \text{(SC7)}$$

Substituting in the *Alk** tracer where possible gives:

$$\frac{\partial A^{s}}{\partial t} + \mathbf{U}\cdot\nabla Alk^{*} + \nabla\cdot(D\nabla Alk^{*}) = SMS(A) \qquad \text{(SC8)}$$

This demonstrates that sources and sinks of alkalinity will also linearly affect *Alk** and is equivalent to the basic conservation equation (SC1) that mixes linearly.

Traditionally salinity normalized potential alkalinity tracer, sA_P:

$$sA_p = 35 \times \frac{A_p}{S} \quad \text{(SC9)}$$

a similar tracer, does not mix conservatively, has a variable response to carbonate production, and has an undefined value for a riverine end-member with zero salinity (Jiang et al., 2014). Figure SC1 shows differences between individual sA_P estimates and the global mean estimate $\overline{sA_p}$ against the differences between individual *Alk** estimates and the global mean estimate $\overline{Alk^*}$. Figure SC1 shows that the *Alk** and sA_P distributions are broadly similar despite these differences in approach, though discrepancies between them are pronounced (>2000 μmol kg^{-1}) where there are large concentrations of riverine water.

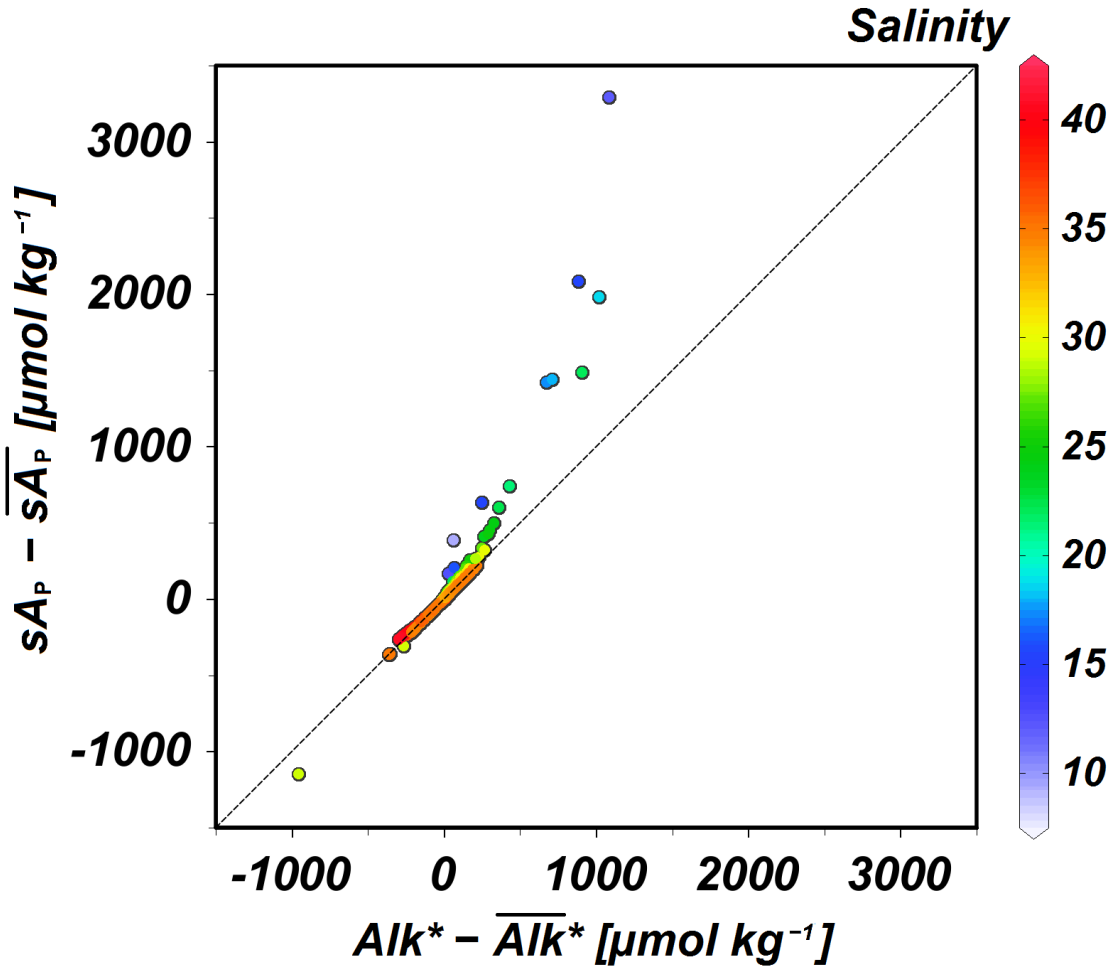

Figure 1. The difference between traditionally normalized potential alkalinity, sA_P, and the mean surface traditionally normalized potential alkalinity, $\overline{sA_P}$, plotted against the difference between *Alk** and the mean surface *Alk**, $\overline{Alk^*}$, for all data in our merged CARINA, PACIFICA, and GLODAP bottle data product. Salinity is indicated by dot color. The vast majority of data fall near the dashed 1:1 line which we provide for reference. However, the large deviations from this line, dominantly in low-salinity Arctic data, reveal the significant differences between the salinity normalization strategies used for *sAp* and *Alk**.

SD: Riverine alkalinity budget is in a separate supplementary materials file in this archive.

SE: Example *M* and *I* calculations for organic matter cycling (*i* = 2) at depth

$$M_2 = \sigma_{R_2} \left| \sum_{j=1}^{7} \frac{\partial \Omega_{\mathrm{C}}}{\partial X_j} \frac{\partial X_{j,2}}{\partial R_i} \right| = \sigma_{R_2} \left| S_{R_2} \right|$$

R_2 is phosphate (P), and the values of the various terms are from Table 1 and A1. If we remineralize σ_{R_2} µmols/kg of phosphate worth of organic matter, this…

$$\begin{aligned} M_i = 0.60\ \mu\text{mol P/kg} \Bigg| & \left(0 \frac{1}{\text{db}} \times -0.00028 \frac{\text{db}}{\mu\text{mol P/kg}} \right) + && \text{... has no effect on pressure} \\ & + \left(0 \frac{1}{^\circ\text{C}} \times 0.014 \frac{^\circ\text{C}}{\mu\text{mol P/kg}} \right) + && \text{... has no effect on temperature} \\ & + \left(0 \times -0.011 \frac{1}{\mu\text{mol P/kg}} \right) + && \text{... has no effect on salinity} \\ & + \left(1 \frac{1}{\mu\text{mol P/kg}} \times -0.0085 \frac{\mu\text{mol P/kg}}{\mu\text{mol P/kg}} \right) + && \text{... increases phosphate} \\ & + \left(0 \frac{1}{\mu\text{mol Si/kg}} \times -0.00012 \frac{\mu\text{mol Si/kg}}{\mu\text{mol P/kg}} \right) + && \text{... has no affect on silicate (soft tissue pump only)} \\ & + \left(-20.16 \frac{1}{\mu\text{mol } A_{\mathrm{T}}\text{/kg}} \times 0.0082 \frac{\mu\text{mol } A_{\mathrm{T}}\text{/kg}}{\mu\text{mol P/kg}} \right) + && \text{... decreases alkalinity by } 1.26 \times 16 \times \text{(phosphate change)} \\ & + \left(117 \frac{1}{\mu\text{mol } C_{\mathrm{T}}\text{/kg}} \times -0.0079 \frac{\mu\text{mol } C_{\mathrm{T}}\text{/kg}}{\mu\text{mol P/kg}} \right) \Bigg| && \text{... increases } C_{\mathrm{T}} \text{ according to the remineralization ratio} \\ = 0.66 & \end{aligned}$$

This *M* value corresponds to an *I* value of…

$$I_i = 100\% \times \frac{M_i}{\sum_{i=1}^{6} M_i}$$

$$I_2 = 100\% \times \frac{M_2}{M_1 + M_2 + M_3 + M_4 + M_5 + M_6}$$

$$I_2 = \frac{100\% \times 0.66}{0.23 + 0.66 + 0.011 + 0.4 + 0.06 + 0.017} = 48\%$$

References for Supplementary Materials

Antonov, J. I., D. Seidov, T. P. Boyer, R. A. Locarnini, A. V. Mishonov, H. E. Garcia, O. K. Baranova, M. M. Zweng, and D. R. Johnson (2010), World Ocean Atlas 2009, Volume 2: Salinity. S. Levitus, Ed. NOAA Atlas NESDIS 69, U.S. Government Printing Office, Washington, D.C., 184 pp.

Dickson, A.G., C.L. Sabine, and J.R. Christian (Eds.) 2007. Guide to best practices for ocean CO_2 measurements. PICES Special Publication 3, 191.

Garcia, H. E., R. A. Locarnini, T. P. Boyer, J. I. Antonov, O. K. Baranova, M. M. Zweng, and D. R. Johnson (2010), World Ocean Atlas 2009, Volume 3: Dissolved Oxygen, Apparent Oxygen Utilization, and Oxygen Saturation. S. Levitus, Ed. NOAA Atlas NESDIS 70, U.S. Government Printing Office, Washington, D.C., 344 pp.

Garcia, H. E., R. A. Locarnini, T. P. Boyer, J. I. Antonov, M. M. Zweng, O. K. Baranova, and D. R. Johnson (2010), World Ocean Atlas 2009, Volume 4: Nutrients (phosphate, nitrate, silicate). S. Levitus, Ed. NOAA Atlas NESDIS 71, U.S. Government Printing Office, Washington, D.C., 398.

Jiang, Z. P., T. Tyrrell, D.J. Hydes, M. Dai, and S.E. Hartman (2014), Variability of alkalinity and the alkalinity-salinity relationship in the tropical and subtropical surface ocean. *Global Biogeochem. Cycles*, *28*(7), 729-742, doi: 10.1002/2013GB004678.

Locarnini, R. A., A. V. Mishonov, J. I. Antonov, T. P. Boyer, H. E. Garcia, O. K. Baranova, M. M. Zweng, and D. R. Johnson (2010), World Ocean Atlas 2009, Volume 1: Temperature. S. Levitus, Ed. NOAA Atlas NESDIS 68, U.S. Government Printing Office, Washington, D.C.,

184 pp.

Schlitzer, R. (2012), Ocean Data View, http://odv.awi.de.